VIIRS Reflective Solar Bands On-Orbit Calibration Using Solar Diffuser and Solar Diffuser Stability Monitor

Junqiang Sun[1,2] and Menghua Wang[1]

[1]NOAA/NESDIS Center for Satellite Applications and Research,
5830 University Research Ct., College Park, MD 20740, USA
[2]Global Science and Technology, Inc., 7855 Walker Drive, Suite 200, Greenbelt, MD 20770, USA

ABSTRACT

The reflective solar bands (RSB) of the Visible Infrared Imaging Radiometer Suite (VIIRS) on board the Suomi National Polar-orbiting Partnership (SNPP) satellite are primarily calibrated on-orbit by a solar diffuser (SD) panel whose performance is monitored by an accompanying solar diffuser stability monitor (SDSM). In this paper, the SD and SDSM calibration methodology is reviewed and the results from the analysis of the up-to-date three and half years of mission data are presented. With the newly derived product of the SD bidirectional reflectance factors, the vignetting functions for the screens in the SD/SDSM system and the carefully selected "sweet spots", and the fully illumination region, the artificial seasonal patterns and noises in the derived SD degradation and the RSB calibration coefficients are removed or significantly reduced. The result shows that the SD degrades faster at short wavelengths while the RSB degrades in a much complex pattern.

***Index Terms*—** VIIRS, RSB, SD, SDSM, Calibration

1. INTRODUCTION

The Visible Infrared Imaging Radiometer Suite (VIIRS) on-board the Suomi National Polar-orbiting Partnership (SNPP) satellite was successfully launched on October 28, 2011 [1, 2]. VIIRS has 22 spectral bands covering a spectral range from 0.410 to 12.013 μm. Among them, fourteen are Reflective Solar Bands (RSB). The VIIRS RSB are calibrated on orbit using an on-board Solar Diffuser (SD) [3-5] with its degradation tracked by a Solar Diffuser Stability Monitor (SDSM) [6-8]. The VIIRS RSB on-orbit changes are also monitored with scheduled monthly lunar observations through the instrument's Space View (SV) [9]. The high accuracy and both short-term and long-term stability of the calibration coefficients are especially important for VIIRS ocean color Environmental Data Records (EDR) [10, 11].

We focus on the VIIRS RSB calibration using SD observations and SDSM measurements in this paper. Figure 1 is a schematic diagram of the SD/SDSM calibration. The

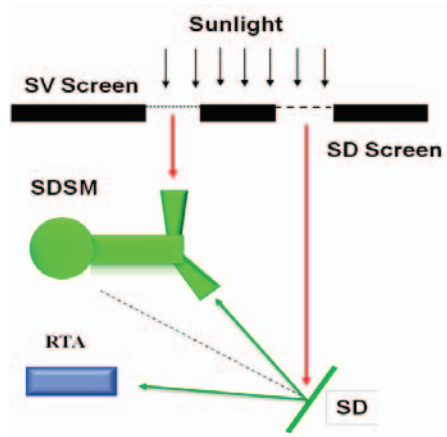

Fig. 1. VIIRS SD and SDSM calibration.

accuracy of the RSB calibration using the SD as well as the SD degradation tracking using the SDSM depends on that of the bidirectional reflectance factors (BRFs) of the SD for both the RSB and the SDSN views and also on the vignetting functions (VFs) of the screens placed in the front of the SD port and SDSM sun view port, through which the SD and SDSM are illuminated by the Sun, respectively. We have carefully derived the BRFs and the VFs [12], with which the seasonal oscillations in both the SD degradation, called H-factors, and the RSB calibration coefficients, called F-factors, are removed and the noises in both of them are significantly reduced. We have also carefully selected the so called "sweet spots", which are fully illumination regions, for both SDSM and SD calibrations. This further improves the quality of the derived H and F-factors. The time-dependent RSR has also applied in this analysis. With the latest and the optimal results of the essential input ingredients as mentioned, the SD calibration can provide smooth, stable, and robust calibration coefficients for the VIIRS RSB. Nevertheless, there are still challenge issues in the VIIRS RSB calibration such as the non-uniformity of the SD degradation, which may induce non-negligible errors in the calibration coefficients of the short wavelength bands.

In this paper, we review the algorithms of the VIIRS SDSM and SD calibration algorithms, show the trending results of the SD degradation and RSB calibration coefficients, derived from the SD/SDSM measurements, and

discuss the challenge issues related to the RSB calibration. In Section 2, the SDSM calibration algorithms are reviewed and the SD degradation results are shown. The SD degradation is strongly wavelength dependent and the SD degrades much faster at the short wavelength. In Section 3, the SD calibration algorithms are reviewed and the RSB F-factors derived from the SD calibration are displayed. The changes of the RSB calibration coefficients with time are also strongly wavelength dependent. The largest change of the calibration coefficients occurs at the near-infrared (NIR) range, while those of the short wavelength bands have much smaller change. Section 4 summarizes and concludes the work.

2. SDSM CALIBRATION

2.1. Algorithms

The SNPP VIIRS SDSM shown in Fig. 1 is a ratio radiometer, consisting of a spherical integrating sphere (SIS) with a single input aperture and eight filtered detectors. The center wavelengths of the eight SDSM detectors are listed in Table 1. The SDSM views the SD, Sun, and the dark scene inside the SDSM. In the SDSM calibration methodology, a linear approximation is applied to establish the relationship between the radiance of the incident sunlight at the center wavelength of SDSM detector d and the background-subtracted digital count dc_D from the detector. Both the SD through the SD port and the SDSM entrance aperture through the SD sun-view port are fully illuminated during a short window, called "sweet spots", of time when the satellite approaches the South Pole from the night side of the Earth and only the data in the "sweet spots" can be used to derive the SD degradation.

The SD degradation at the center wavelength, λ_D, of the SDSM detector D can be tracked by the ratio of the detector's SD view response to its sun view response [8], i.e.

$$H(\lambda_D) = \left\langle \frac{dc_{SD,D}}{\rho_{SD,SDSM}(\lambda_D)\tau_{SDS}\cos(\theta_{SD})} \right\rangle \Big/ \left\langle \frac{dc_{SV,D}}{\tau_{SVS}} \right\rangle, \quad (1)$$

where $dc_{SD,D}$ and $dc_{SV,D}$ are background-subtracted SD view response of the SDSM detector D, respectively, $\rho_{SD,SDSM}(\lambda_D)$ is the BRF with outgoing direction toward the SDSM for the detector before the SD started to degrade on-orbit, τ_{SDS} and τ_{SVS} are the VF of the SD port screen and SDSM sun view port screen, respectively, θ_{SD} is the solar-zenith angle to the SD, and <…> indicates the average over the 'sweet spots", which are slight different for SD view and SDSM view.

2.2. SD Degradation

SNPP VIIRS SDSM calibration was performed in every orbit, generating about 14 events every day in the first few months on orbit, then the operational rate was reduced to once per day, and further reduced to once per two days after May 16, 2014. The on-orbit SD degradations derived from SDSM measurements via Eq. (1) at the wavelengths of the SDSM detectors are shown in Fig. 2 in symbols. The first set of SDSM measurements was made on November 8, 2011 when the SNPP VIIRS was turned on after 11 days on orbit. The nadir door was opened on November 21, 2011. The SD degradation shows the expected result that the degree of degradation is greater at short wavelengths. In the past three plus years since the VIIRS has gone on-orbit, the SD has degraded about 29.5%, 23.5%, 18.0%, 11.4%, 4.9%, 3.2%, 1.8%, and 1.3% at wavelengths of 412, 450, 488, 555, 672, 746, 865, and 935 nm, respectively.

The SD degrades with time in the first two years but with changing degradation rate as expected. Unexpectedly, the SD reflectance started to increase on February 5, 2014 and this trend lasted for about 75 days before reverting back, but no longer following the expected declining pattern. This unexpected SD reflectance change for VIIRS signals a different physical or chemical change of the SD surface that shortly dominated the degradation of the SD surface.

Table 1. Specification for SNPP VIIRS RSB and SDSM detectors.

VIIRS Band	CW* (nm)	Band Gain	SDSD Detector	CW* (nm)
M1	410	DG	D1	412
M2	443	DG	D2	450
M3	486	DG	D3	488
M4	551	DG	D4	555
I1	640	SG	NA	NA
M5	671	DG	D5	672
M6	745	SG	D6	746
M7	862	DG	D7	865
I2	862	SG	D7	865
NA	NA	N	D8	935
M8	1238	SG	NA	NA
M9	1378	SG	NA	NA
M10	1610	SG	NA	NA
I3	1610	SG	NA	NA
M11	2250	SG	NA	NA

*CW: Center Wavelength; DG: Dual Gain; SG: Single Gain

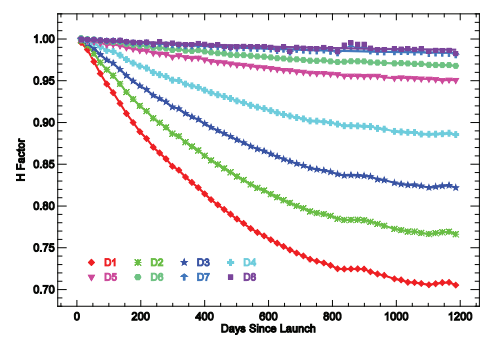

Fig. 2. SD degradation derived from SDSM calibration.

The results in Fig. 2 demonstrate that the SD degradation can be accurately tracked by the SDSM calibration. However, it is worth to mention that the SDSM catches, in principle, the SD degradation for the outgoing direction toward the SDSM view direction. With the assumption that the SD degrades uniformly with the incident and outgoing directions, the SD degradation derived from the SDSM calibration can be applied in the SD calibration to derive the RSB calibration coefficients. Since the SD degradation is derived from the SDSM calibration only at 8 wavelengths, linear interpolation between adjacent pairs is used to obtain the SD degradation at other wavelengths.

We have demonstrated in our previous work [8] that the SD degrades non-uniformly, especially at wavelengths of the short wavelength bands. The non-uniformity of the SD degradation may bring some errors for short wavelength bands when the SD degradation derived from the SDSM for the SDSM view to the RSB view. The SDSM also has no capability to catch the SD degradation for the wavelength range of the shortwave infrared (SWIR) bands. Currently, it is assumed that the SD has no degradation at the SWIR wavelengths when the SD result is applied to calibrate the SWIR bands.

3. SD CALIBRATION

3.1. Algorithms

The VIIRS SD is made of Spectralon®, installed inside the instrument, and used as a reference to calibrate the VIIRS RSB. The center wavelengths of the RSB are listed in Table 1. In the VIIRS RSB radiance retrieval methodology, a quadratic approximation is applied to establish the relationship between the radiance of the incident sunlight at the center wavelength of a detector of a RSB and the background-subtracted digital number *dn* of the detector. The SD through the SD port is fully illuminated during a short window of time, called "sweet spot", when the satellite approaches the South Pole from the night side of the Earth and only the data in the "sweet spot" are used to derive the RSB calibration coefficients.

The calibration coefficients, F-factors, for a RSB using the SD observation can be calculated by [5]

$$F(B,D,M,G) = \frac{RVS_{B,SD} \cdot \int RSR_B(\lambda) \cdot L_{SD}(\lambda) \cdot d\lambda}{\sum_i c_i(B,D,M,G) dn^i \cdot \int RSR_B(\lambda) \cdot d\lambda}, \quad (2)$$

where B, D, M, and G are band number, detector number, mirror side of the half angle mirror, gain status of the band, respectively. $RVS_{B,SD}$ is the response versus scan angle (RVS) at AOI of SD for band B, RSR_B is time-dependent relative spectral response (RSR) of the band. $c_0(B,D,M,G)$, $c_1(B,D,M,G)$, and $c_2(B,D,M,G)$ are the temperature effect corrected prelaunch calibration coefficients, and dn is the background subtracted instrument response of band B detector D when view the SD. In Eq. (2), $L_{SD}(\lambda)$ is the radiance of the sunlight reflected by the SD and can be expressed as

$$L_{SD}(\lambda) = I_{Sun}(\lambda) \cdot \tau_{SDS} \cdot \cos(\theta_{SD}) \cdot BRF_{RTA} \cdot h(\lambda) / d_{VS}^2, \quad (3)$$

where I_{Sun} is solar irradiance, BRF_{RTA} is the bidirectional reflectance factor for the outgoing direction of the rotating telescope assebly (RTA) via which the RSB views the earth view (EV), the SV, the SD, and other on-baord calibrators. $h(\lambda)$ is the on-orbit SD degrdation tracked by the SDSM and normalized on October 28, 2011, and d_{VS} is VIIRS-Sun distance. The BRF, VF, and $\cos(\theta_{SD})$ describe the dependence of the reflected solar radiance on the solar angles. The BRF and VF were measured prelaunch and validated on-orbit using the on-orbit measurements from the planned yaw maneuvers. The F-factors derived using Eq. (2) are averaged over scans and samples in the "sweet spot".

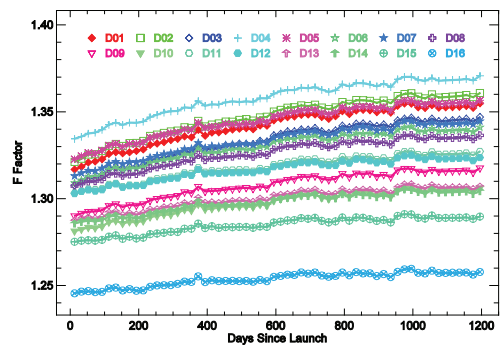

Fig. 3. VIIRS band M1 (410 nm) F-factors.

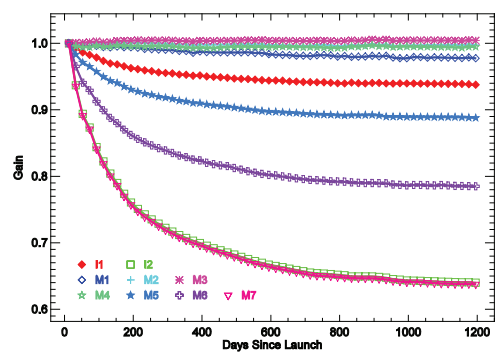

Fig. 4. VIIRS band averaged F-factors.

3.2. RSB Calibration Coefficients

SNPP VIIRS SD calibration is performed in every orbit generating about 14 events every day. Figure 3 shows the RSB calibration coefficients, i.e., F-factors, derived from the SD calibration for VIIRS band M1 (410 nm). No seasonal oscillations or random jumps are seen in the derived F-factors, which are in fact very stable. The band averaged

gains, which is inversely proportional to band averaged F-factors, for the RSB are shown in Fig. 4. The degradation is strongly band or wavelength dependent. The largest gain degradation occurs at the NIR band I2 and M7, both of which have same wavelength of 862 nm, while the degradations of the short wavelength bands are much smaller. This is very different from the Moderate Resolution Imaging Spectroradiometer (MODIS) RSB for which the largest degradation occurs at short wavelength bands. The gains of bands I2 and M7 have degraded about 36%, equivalent to a 56% increase of the F-factors as shown in Fig. 4, since launch on October 28, 2014, while the degradation for bands M1, M2, M3, and M4 are less than 2.2%, respectively. Band M3 has the least degradation. For VIIRS RSB, there are two main competing mechanisms for RSB gain degradation. One is half angle scan mirror (HAM), which may degrade more at short wavelengths, same as for the MODIS scan mirror. This is why band M1 has the largest degradation, then M2, and finally M3. Since there is a RTA in front of the scan mirror, the HAM mirror has degraded much less than the scan mirror of either MODIS instrument. Thus, the VIIRS short wavelength bands have much less degradations in last almost three years. Another mechanism is the degradation of the RTA. It is known that it degrades the fastest at the NIR range, while its degradation at visible range is much smaller.

Consistent with the observation in the SDSM measurements, then non-uniformity of the SD degradation of SD with respect to both the incident and the outgoing directions has also been observed in the RSB measurements, especially in short wavelength spectral region. This means that the SD degradation can be different for the SDSM view and the RSB view. It was estimated that the direct application of the SD degradation derived from the SDSM measurements as the SD degradation for the RSB view can bring in non-negligible errors in the F-factors and then in EDR ocean color products [11] for the short wavelength visible bands. A mitigation approach based on both the SDSM and lunar calibration has been developed [5], and it has been demonstrated that this approach can remove the errors due to non-uniformity of the SD degradation [11].

4. SUNMARY

We have reviewed the on-orbit VIIRS RSB calibration using the SD/SDSM and showed the updated results for the three plus years since VIIRS launch. The updated results show that the calibration methodology is working as expected with carefully derived BRFs for the SD and the VFs for the screens in the SD/SDSM system and proper selected "sweet spots". Both the SD degradation and the RSB calibration coefficients are strongly wavelength dependent as expected. For the SD degradation, the lager degradation occurs at the shorter wavelength bands. For the RSB calibration coefficients, the largest degradation appears at VIIRS bands I2 and M7, while the short wavelength bands have much less degradation in the last three plus years. The non-uniformity of the SD degradation may bring non-negligible errors in the F-factors derived from the SD/SDSM calibration for short wavelength bands.

ACKNOWLEDGMENTS

This work was supported by JPSS/VIIRS funding. The views, opinions, and findings contained in this paper are those of the authors and should not be construed as an official NOAA or U.S. Government position, policy, or decision.

REFERENCES

[1] C. Cao, et al, "Early on-orbit performance of the Visible Infrared Imaging Radiometer Suite (VIIRS) onboard the Suomi National Polar-orbiting Partnership (S-NPP) satellite," *IEEE Trans. Geosci. Remote Sens.*, 52, 1142–1156 (2014).

[2] Xiong, et al, "VIIRS on-orbit calibration methodology and performance," *J. Geophys. Res. Atmos*., 119, 5065–5078 (2014).

[3] N. Lei, et al, "Initial on-orbit radiometric calibration of the Suomi NPP VIIRS reflective solar bands," *Proc. SPIE*, 8510, 851018 (2012).

[4] C. Cardema, et al, "Operational calibration of VIIRS reflective solar band sensor data records," *Proc. SPIE*, 8510, 851019 (2012).

[5] J. Sun and M. Wang, "VIIRS Reflective Solar Bands On-Orbit Calibration and Performance: A Three-Year Update," *Proc. SPIE*, 9264, 92640L (2014).

[6] J. Fulbright, et al, "Characterization and performance of the Suomi-NPP VIIRS solar diffuser stability monitor," *Proc. SPIE*, 8510, 851015 (2014).

[7] E. Hass, et al, "VIIRS solar diffuser bidirectional reflectance distribution function (BRDF) degradation factor operational trending and update," *Proc. SPIE*, 8510, 851016 (2012).

[12] J. Sun and M. Wang, "Visible Infrared Imaging Radiometer Suite solar diffuser calibration and its challenges using a solar diffuser stability monitor," *Appl. Opt.* **53**, 8571–8584 (2014).

[9] J. Sun, X. Xiong, and J. Butler, "NPP VIIRS on-orbit calibration and characterization using the moon," *Proc. SPIE*, 8510, 85101I, 2012.

[10] M. Wang, "Remote sensing of the ocean contributions from ultraviolet to near-infrared using the shortwave infrared bands: simulations," Appl. Opt., 46, 1535–1547 (2007).

[11] M. Wang, et al, "Evaluation of VIIRS ocean color products," *Proc. SPIE,* 9261, 92610E (2014).

[12] J. Sun and M. Wang, "On-orbit characterization of the VIIRS solar diffuser and solar diffuser screen," *Appl. Opt*., 54, 236-252 (2015).